Journal of Alloys and Compounds 509 (2011) 1482–1488

Contents lists available at ScienceDirect

Journal of Alloys and Compounds

journal homepage: www.elsevier.com/locate/jallcom

Solvothermal synthesis and characterization of tungsten oxides with controllable morphology and crystal phase

Jing-Xiao Liu[a,b,*], Xiao-Li Dong[b], Xiang-Wen Liu[a], Fei Shi[b], Shu Yin[a], Tsugio Sato[a]

[a] Institute of Multidisciplinary Research for Advanced Material, Tohoku University, Sendai 980-8577, Japan
[b] School of Chemistry and Materials, Dalian Polytechnic University, Dalian 116034, PR China

ARTICLE INFO

Article history:
Received 13 August 2010
Received in revised form 2 October 2010
Accepted 11 October 2010
Available online 21 October 2010

Keywords:
Oxide materials
Chemical synthesis
Optical properties
Scanning electron microscopy

ABSTRACT

Tungsten oxides with various morphologies and crystal phases were synthesized by solvothermal reactions at 200 °C for 7–12 h using different solvents. The morphology and crystal phase of tungsten oxides changed depending on the solvents, i.e., spherical particles of ca. 1 μm in diameter consisting of nanowires, spindle shaped bundles of ca. 1 μm in length consisting of nanowires and accumulations consisting of micrometer sized plates and/or rods of tungsten oxides were obtained using ethanol, 1-propanol and water–ethanol mixed solution, respectively. When water–ethanol mixed solution was used, the crystallinity of tungsten oxide increased but the specific surface area greatly decreased. Crystallinity of tungsten oxides had more important effects on the NO degradation under light irradiation. The product using 42.9 vol.% water–ethanol mixed solvent consisted of the mixture of anhydrous tungsten oxide and hydrous tungsten oxide with preferential orientation of (0 0 2) plane and small band gap energy (2.43 eV), and showed higher photocatalytic degradation of NO even though it had a much smaller specific surface area than those prepared using ethanol and 1-propanol.

1. Introduction

Tungsten oxide (WO_3), an n-type semiconductor metallic oxide, has many unique characteristics such as electrochromic [1], photoelectrochemical [2], photocatalytic activities [3] and gas sensing effects [4]. It was also reported that the dispersions of reduced tungsten oxide showed a remarkable absorption of near infrared light while retaining a high transmittance of visible light and this property is highly suitable for solar control filters in automotive and architectural windows [5]. As gas sensors, tungsten oxides have been studied to detect NO_x [6,7], NH_3 [8,9], H_2S [10], ethylene [11] and other VOC gases [12]. Since tungsten oxide possesses a small band gap energy of 2.4–2.8 eV, it has the potential ability of photocatalysis under irradiation of visible light [13]. It was reported that WO_3 loaded with nanoparticulate of Pt and Pd exhibited high photocatalytic activity under visible light irradiation for the decomposition of organic compounds [14–16]. It was also found that WO_3/TiO_2 nanocomposites have increased photocatalytic activity than that of pure TiO_2 [17]. Up to now, tungsten oxides as photocatalysis materials have been studied extensively [18–20], even though pure WO_3 has lower light energy conversion efficiency than the more widely used TiO_2 due to its low conduction band level.

As is well known, the morphology and microstructure of particles have a great effect on the properties. Recently, the morphology controlled synthesis of tungsten oxide particles has attracted considerable attention [21–23]. One-dimensional (1D) tungsten oxides especially have attracted considerable interest due to their high aspect-ratio structure, large surface areas and unique physical properties, including optical, electronic characteristics and gas sensing effects [24–26]. Among the various synthesis methods of tungsten oxide nanoparticles, hydrothermal and solvothermal reaction processes have significant advantages, such as total control over their shape and size, low processing temperature, high homogeneity and so on [27–29]. Especially, the morphology of tungsten oxide could be effectively controlled by the solvothermal synthesis [29]. Since tungsten oxide compound has many crystal structures, the control of morphology and crystal phase maybe play important roles in achieving particular and excellent properties. One-dimensional tungsten oxides such as nanowires and nanorods have been studied extensively. It was reported that hierarchical WO_3 hollow shells with larger surface areas showed enhanced photocatalytic activities for the degradation of organic contaminants under visible light irradiation [30]. However, the relationship among the crystal phase, morphology, optical absorption and photocatalysis of tungsten oxides are rarely systematically investigated.

* Corresponding author at: School of Chemistry and Materials, Dalian Polytechnic University, #1 Qinggongyuan, Dalian 116034, PR China. Fax: +86 0 411 86323736.
E-mail addresses: drliu-shi@dlpu.edu.cn, jxiaoliu@sina.com (J.-X. Liu).

0925-8388/$ – see front matter © 2010 Elsevier B.V. All rights reserved.
doi:10.1016/j.jallcom.2010.10.052

In this article, tungsten oxides with different morphologies and crystal phases were synthesized by the solvothermal reaction, and the optical absorption and photocatalysis properties of them were studied accordingly; meanwhile, the relationship among them was also investigated and discussed. The obtained results may be significant for morphology and phase controllable synthesis of Pt-loaded WO_3 with high photocatalysis in the next study.

2. Experimental

2.1. Synthesis of tungsten oxide particles

Tungsten hexachloride (WCl_6, purity 90%, Kanto Chemical Co, Inc.) was used as raw material. Ethanol (purity 99.5%), 1-propanol (purity 99.5%) and water–ethanol mixed solution were used as solvothermal reaction solvents. The precursor solutions were prepared by dissolving 0.389 g of tungsten hexachloride in 70 ml of ethanol, 1-propanol and water–ethanol mixed solution with stirring. When water–ethanol mixed solution was used, 0.389 g of tungsten hexachloride was firstly dissolved in a certain amount of ethanol, and then a certain amount of water was added to the solution under stirring. In this work, the water content in water–ethanol mixed solution was adjusted as 8.57, 42.9 and 85.7 vol.%. The final concentration of WCl_6 in each solution was 0.014 M.

After transferring the precursor solution into a Teflon®-lined autoclave with 100 ml of internal volume, solvothermal reaction was conducted at 200 °C for 7–12 h in an electric oven. The obtained solid precipitates were then centrifuged and washed with ethanol three times followed by vacuum drying at 60 °C overnight.

2.2. Characterization

The phase compositions of the samples were determined by X-ray diffraction analysis (XRD, Shimadzu XD-D1) using graphite-monochromized CuKα radiation. The specific surface areas were determined by nitrogen adsorption–desorption isotherm measurement at 77 K (BET, Quantachrome NOVA-4200e). The morphology and microstructures of the samples were observed by a scanning electron microscopy (SEM, HITACHI S-4800) and a transmission electron microscopy (TEM, JEOL JEM-2010). The diffuse reflectance spectra of ultra violet–visible light were measured by UV-visible spectrophotometer (JASCO V-670 spectrophotometer) and the band gap was determined from the onset of the spectrum.

The photocatalytic activity of the obtained tungsten oxide was evaluated by measuring the oxidative destruction ability of nitrogen monoxide using a flow-type reactor as reported in the literature [31,32]. The tungsten oxide powder sample was placed in a hollow of 20 mm length × 16 mm width × 0.5 mm depth on a glass holder plate and set in the bottom center of the reactor box. A 450 W high-pressure mercury lamp was used as the light source. The irradiation light wavelength was controlled by various filters, i.e., Pyrex glass for cutting off the light of wavelength <290 nm, Kenko L41 Super Pro (W) filter <400 nm and Fuji triacetyl cellulose filter <510 nm. A NO/air mixed gas with 1 ppm NO and 50 vol.% air (balance nitrogen) was flowed into the reactor at a flowing rate of 200 cm^3/min. The concentration of NO gas was measured at the outlet of the reactor box (373 cm^3).

3. Results and discussion

3.1. Morphology

Figs. 1 and 2 show the SEM micrographs of the as-synthesized products with different solvents at 200 °C for 7 h and 12 h, respectively. When ethanol was used as a solvent, urchin-like spheres of ca. 1 μm in diameter consisted of nanowires were formed (Figs. 1a and 2a). They were very like the images of h-WO_3 synthesized from sodium tungstate reported in the literature [25,28]. The nanowires in the spherical particles in Fig. 2a were thicker than those in Fig. 1a, indicating that the diameter of nanowire increased with time due to the grain growth. When 1-propanol was used as a solvent, spindle shaped bundles of ca. 1 μm in length and 50–100 nm in diameter consisting of nanowires were formed (Figs. 1b and 2b).

In water–ethanol mixed solutions, accumulations consisting of micrometer sized plates and rods were formed. The products synthesized at 200 °C for 7 h using 8.57 vol.% water–ethanol mixed solution consisted of the hexagonal plates of 2–5 μm in diameter (see Fig. 1c), while the product with 42.9 vol.% water for 12 h showed a kind of composite consisting of microplates of ca. 5–10 μm in diameter and microrods of 10–20 μm in length and 1–2 μm in diameter (see Fig. 2c). As for the products with 85.7 vol.% water–ethanol mixed solution, the morphologies changed with reaction time, i.e., with increasing the reaction time from 7 to 12 h, the products changed from mixture of accumulations of microrods and irregular plate-like particles to those of thinner plate-like particles (see Figs. 1d and 2d).

Fig. 3 shows the TEM images of products synthesized by the solvothermal reactions at 200 °C for 12 h with ethanol and 1-propanol. It was clearly seen that the urchin-like spherical particles formed in ethanol consisted of nanowires of 200–500 nm in length and 10–20 nm in diameter. In contrast, the spindle shaped bundles formed in 1-propanol consisted of nanowires of 10–20 nm in diameter.

On the basis of the obtained various morphology of tungsten oxides, it can be concluded that the components of solvent played an important role in the morphology. Pure organic solvents such as ethanol and 1-propanol facilitated the formation of nanowires, although the formation mechanism of urchin-like spheres with ethanol and spindle shaped bundles consisting of nanowires with 1-propanol is not very clear up to now. As for the pure ethanol solvent, it is considered that WCl_6 first dissolves in ethanol to form a 6-fold coordinated $[WCl_m(OC_2H_5)_{6-m}]^{2-}$ complex species and HCl [33]. The linking between the complex species is carried out to form WO_3 by a condensation reaction in the solvothermal process. In the initial period, a large amount of small $[WCl_m(OC_2H_5)_{6-m}]^{2-}$ clusters aggregate to form solid spheres due to homogeneous nucleation and aggregation growth. Due to the absence of oxygen during the solvothermal reaction, the growth of WO_3 along some crystal face was retarded, thus it was more possible to form WO_3 nanowires.

As the amount of water in mixed solvent increases, the mole fraction of oxygen in the tungsten oxide system also increases because water is a source of oxygen in the solvothermal reaction. With the increasing of water content in solvent, the particle shape changed from urchin-like spheres and spindle-like bundles consisting of nanowires to plate-like particles, which is similar to the report by Choi et al. [27].

3.2. Crystalline phase

Fig. 4 shows the XRD patterns of the products by solvothermal reactions at 200 °C for 7 h with different solvents. Before the solvothermal reaction the precursor solution had been aged for 16 h. It is observed that the products synthesized by using ethanol or 1-propanol showed only one weak diffraction peak around $2\theta = 23°$. In contrast, the products with water–ethanol mixed solution showed sharp diffraction peaks as expected by the SEM observation. The product with 8.57 vol.% and 85.7 vol.% water–ethanol mixed solution consisted of single phase orthorhombic $WO_3(H_2O)_{0.333}$ (JCPDS 87-1203, with lattice constants $a = 7.3447$, $b = 12.547$, $c = 7.7367$) and monoclinic WO_3 (JCPDS 89-4476, with lattice constants $a = 7.3237$, $b = 7.5644$, $c = 7.7274$), respectively. These results suggested that with an increase in water content in ethanol–water mixed solution the synthesized product tended to change from hydrous $WO_3(H_2O)_{0.333}$ to anhydrous WO_3.

Fig. 5 shows the XRD patterns of products by solvothermal reactions with different solvents at 200 °C for 12 h. For the products synthesized by using ethanol or 1-propanol, the XRD patterns in Figs. 4 and 5 are very similar, indicating that the obtained tungsten oxides are amorphous with slight tendency of crystallization. However, when 8.57 vol.% water–ethanol mixed solution was used, only weak peak around $2\theta = 23°$ appeared, which is very different from the XRD pattern of product synthesized at 200 °C for 7 h that is shown in Fig. 4c. The main reason is that the two kinds of samples in Figs. 4c and 5c were obtained by different process. As for the sample in Fig. 4c, the WCl_6 precursor solution had been aged

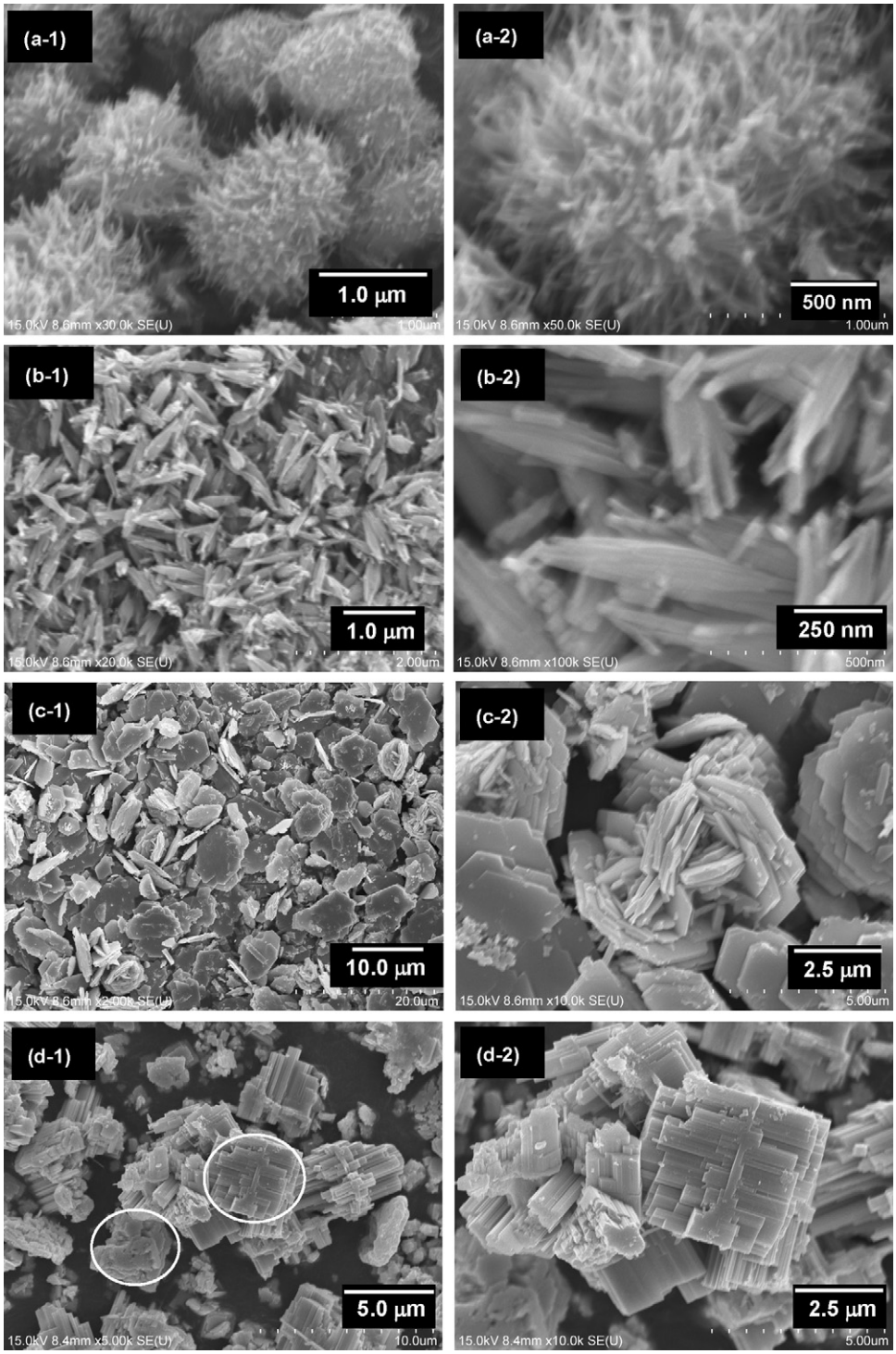

Fig. 1. SEM images of tungsten oxide products by solvothermal reactions at 200 °C for 7 h with different solvents (the precursor solution had been aged for 16 h before solvothermal reaction) (a) ethanol, (b) 1-propanol, (c) 8.57 vol.% water–ethanol mixed solution and (d) 85.7 vol.% water–ethanol mixed solution.

for 16 h before it was transferred into the Teflon®-lined autoclave for solvothermal reaction. During the ageing in the air, some small particles may be formed due to the hydrolysis of WCl_6 with water in the air, which is favorable for obtaining crystal phase with better crystallinity. Therefore, it can be proposed that the pre-ageing of the precursor solution in the air is favorable for obtaining tungsten oxides with better crystallinity.

With the increasing of water content in the solvent, sharp diffraction peaks appeared. For the product with 42.9 vol.% water–ethanol mixed solution, the product consisted of orthorhombic $WO_3(H_2O)_{0.333}$ and monoclinic WO_3 crystal phase (Fig. 5d). In contrast, the product using 85.7 vol.% water–ethanol mixed solution was single phase of monoclinic anhydrated tungsten oxide (WO_3) (Fig. 5e).

In addition, it is found that (0 0 2) peak intensities of $WO_3(H_2O)_{0.333}$ and WO_3 in Figs. 4c,d and 5d,e were higher than the reported values in JCPDS 89-4476 and JCPDS 87-1203, indicating the preferred orientation of the $WO_3(H_2O)_{0.333}$ and WO_3 crystal. These XRD data agreed well with the SEM images, which indicating that the accumulations of rod-like particles and irregular

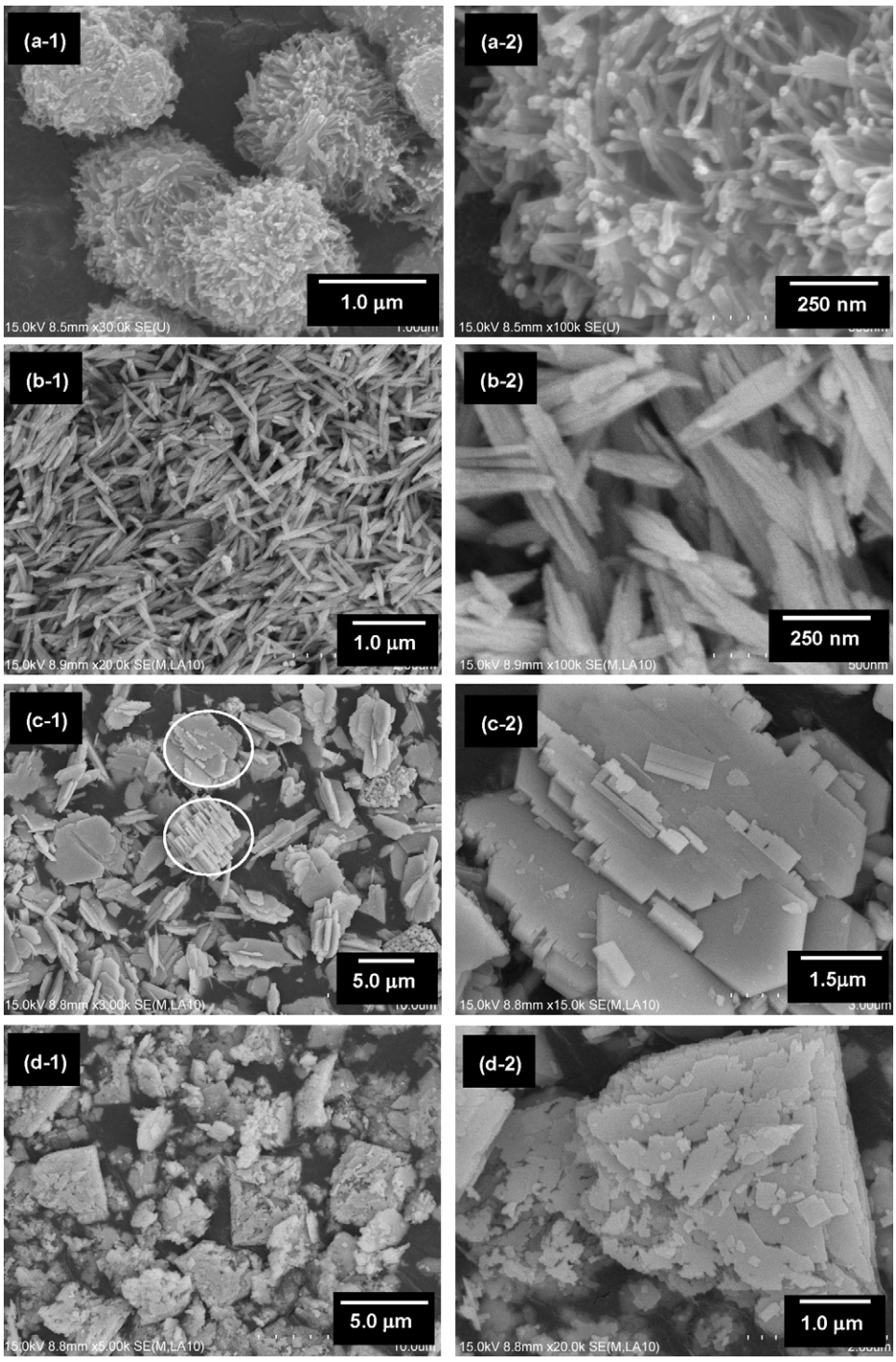

Fig. 2. SEM images of tungsten oxide products by solvothermal reactions at 200 °C for 12 h with different solvents (a) ethanol, (b) 1-propanol, (c) 42.9 vol.% water–ethanol mixed solution and (d) 85.7 vol.% water–ethanol mixed solution.

plate-like particles may be attributed to anhydrated tungsten oxide (WO_3), and the hexagonal plate-like particles may be attributed to hydrated tungsten oxide ($WO_3(H_2O)_{0.333}$), respectively. In addition, it can be seen that anhydrated WO_3 has two kinds of morphologies, which are accumulation of rod-like particles (see Fig. 1d) and plate-like particles (see Fig. 2d). From the XRD and SEM results, it can be concluded that ethanol–water mixed solution with appropriate content of water will lead to formation of plate-like hydrated $WO_3(H_2O)_{0.333}$, whereas the mixed solution with high content of water will lead to formation of accumulations of rod-like or irregular thinner plate-like anhydrated WO_3. The possible reason may be that the water plays an important role in the reaction speed. Due to the thermal decomposition, anhydrated WO_3 should be the final product and hydrated $WO_3(H_2O)_{0.333}$ should be the middle product. With the increasing of water content, the reaction speed tends to be high, so it is more possible to form anhydrated WO_3 by using 85.7 vol.% water–ethanol mixed solution and form intermediate product hydrated $WO_3(H_2O)_{0.333}$ by using 42.9 vol.% water–ethanol mixed solution. Of course, this conjecture needs to be further clarified.

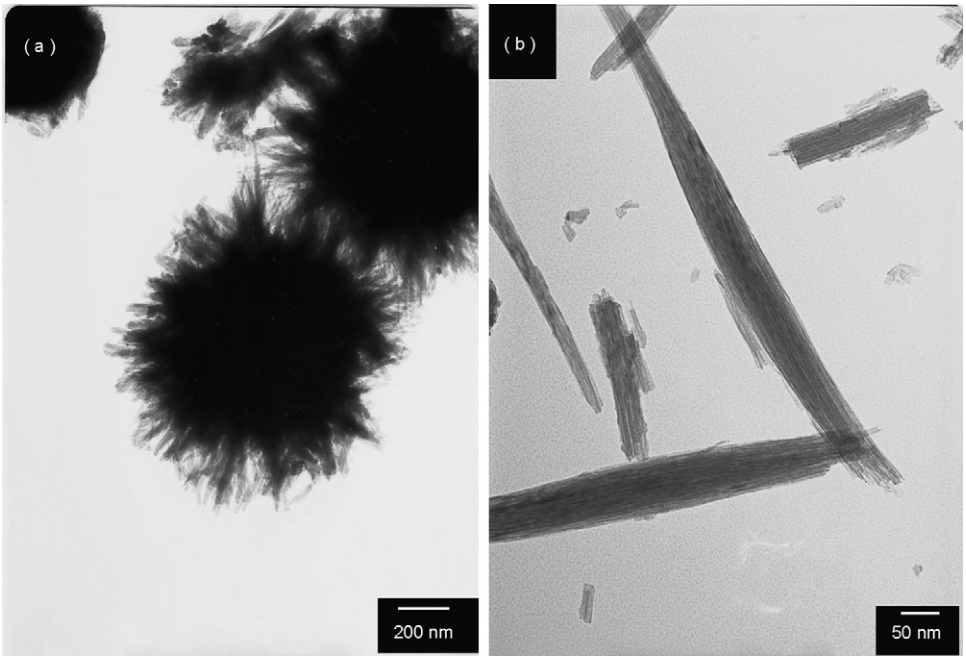

Fig. 3. TEM images of tungsten oxide products by the solvothermal reaction at 200 °C for 12 h with (a) ethanol and (b) 1-propanol.

Fig. 6 shows the diffuse reflection spectra of products by using different solvents. All products showed visible light absorption ability with the onset of absorption around 420–500 nm. The band gap energies (E_g) of the products were determined by Eq. (1)

$$E_g = \frac{1239.8}{\lambda} \quad (1)$$

where λ (nm) is the wavelength of the onset of the spectrum and the results are listed in Table 1 together with the specific surface areas. It was seen that the samples prepared with water–ethanol mixed solutions showed smaller band gap energies and smaller specific surface areas than those prepared with ethanol and 1-propanol. Especially, the specific surface area of product greatly decreased when using water–ethanol mixed solutions because of the promotion of the crystal growth of tungsten oxides as shown in Figs. 1–3.

3.3. Photocatalytic properties

Photocatalytic degradation of NO is of great significance from the viewpoint of practical applications because NO is one of the typical pollutants in the exhaust gases from automobiles. In this work, the destruction of NO was employed as a model reaction to characterize the photocatalytic activity of tungsten oxides. Fig. 7

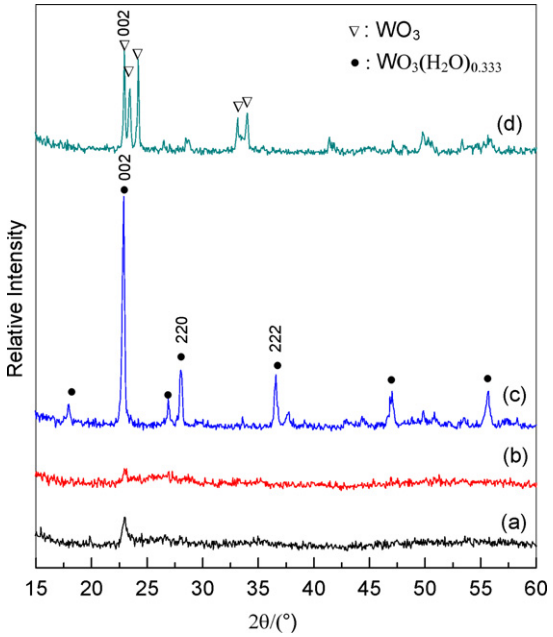

Fig. 4. XRD profiles of tungsten oxide products by solvothermal reactions at 200 °C for 7 h with different solvents (the precursor solution had been aged for 16 h before solvothermal reaction) (a) ethanol, (b) 1-propanol, (c) 8.57 vol.% water–ethanol mixed solution and (d) 85.7 vol.% water–ethanol mixed solution.

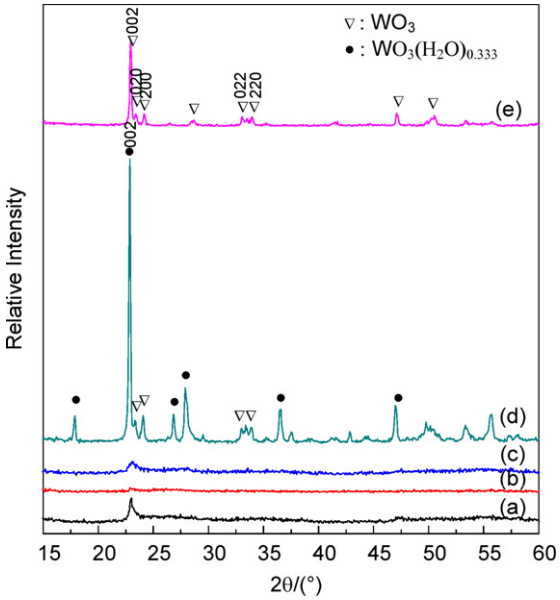

Fig. 5. XRD profiles of tungsten oxide products by solvothermal reactions at 200 °C for 12 h with different solvents (a) ethanol, (b) 1-propanol, (c) 8.57 vol.% water–ethanol mixed solution, (d) 42.9 vol.% water–ethanol mixed solution and (e) 85.7 vol.% water–ethanol mixed solution.

Table 1
Morphology, crystal phase, specific surface area and band gap of the products synthesized by the solvothermal reactions at 200 °C for 12 h with different solvents.

Solvent	Morphology	Crystal phase	Specific surface area (m^2/g)	Band gap (eV)
Ethanol	Urchin like nanowire spheres	Amorphous with slight tendency of crystallization	128.75	2.76
1-Propanol	Spindle shapes nanowire bundles	Amorphous with slight tendency of crystallization	81.42	2.95
42.9 vol.% water–ethanol	Composite morphology with micrometer sized plates and rods	Composite crystals with $WO_3(H_2O)_{0.333}$ and WO_3	3.13	2.43
85.7 vol.% water–ethanol	Accumulations of microrods	WO_3	5.72	2.43

shows the nitrogen monoxide destruction ability of the tungsten oxide powders synthesized with different solvents by solvothermal reaction at 200 °C for 12 h. Although the photocatalytic activity of tungsten oxides is observed to be lower than that of the TiO_2 P25 powder, whereas the differences of photocatalytic degradation of NO for tungsten oxide products synthesized with different solvents is obvious. It can be seen that the samples prepared with water–ethanol mixed solution showed photocatalytic activity under the irradiation of visible light $\lambda > 400$ nm superior to the samples with ethanol and 1-propanol solvents, even though the specific surface area of former sample was much lower than those of latter. In particular, the sample synthesized with 42.9 vol.% water–ethanol mixed solution showed the highest photocatalytic activity in the near ultraviolet light range ($\lambda > 290$ nm). It is known that the photocatalytic activity is closely related to specific surface area and crystallinity, because the high crystallization will have less defects acting as the recombination center and should suppress mutual e^-–h^+ recombination [34]. The effects of specific preferential orientation of crystal faces on the photocatalytic activity of tungsten oxide was reported in the literature [17], in which it was suggested that excellent photocatalytic activity could be obtained by designing and fabricating high regular self-assembled nanoporous WO_3 with preferential orientation of (0 0 2) planes. The products in the present study showed preferential orientation of (0 0 2) planes, and the XRD peak intensity of tungsten oxides prepared in various solvents was in the order of 42.9 vol.% water–ethanol > 85.7 vol.% water–ethanol > ethanol > 1-propanol (see Fig. 5). This order agreed well with the order of photocatalytic activity shown in Fig. 7. It was reported that different crystal plane had different adsorption ability on NO molecules, and the recombination between electrons and holes was difficult to occur on a perfect crystal surface [35]. Although the detail mechanism of preferential orientation of (0 0 2) plane having effects on the NO destruction reaction is not so clear yet, it is obvious that crystallization status of tungsten oxides plays an important role in the photocatalytic activity on the NO destruction in this work.

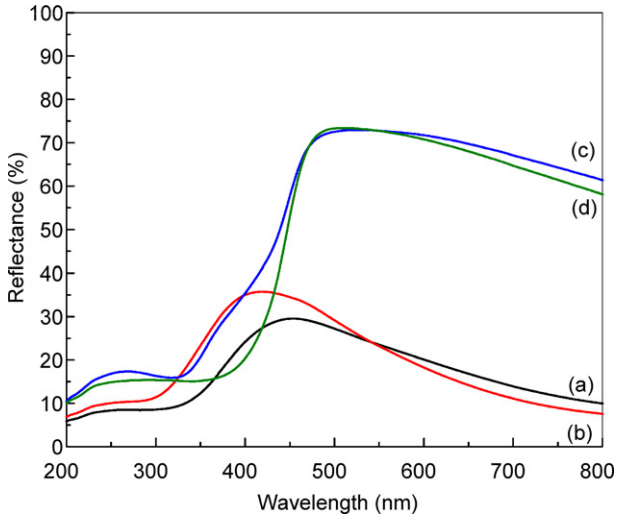

Fig. 6. Diffuse reflectance spectra of products by the solvothermal reactions at 200 °C for 12 h with (a) ethanol, (b) 1-propanol, (c) 42.9 vol.% water–ethanol mixed solution and (d) 85.7 vol.% water–ethanol mixed solution.

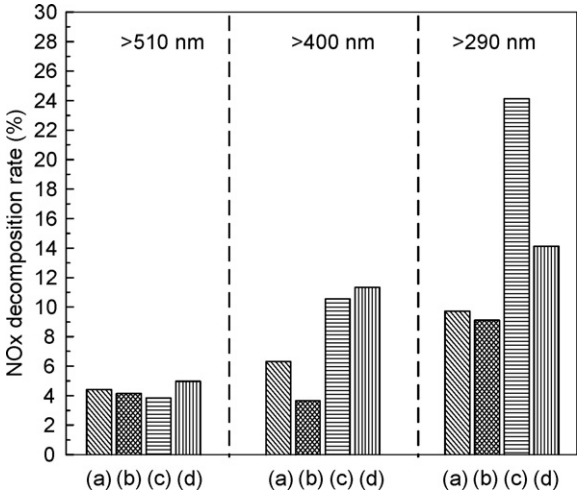

Fig. 7. NO destruction activity of tungsten oxides synthesized by solvothermal reaction at 200 °C for 12 h with (a) ethanol, (b) 1-propanol, (c) 42.9 vol.% water–ethanol mixed solution and (d) 85.7 vol.% water–ethanol mixed solution.

It was also notable that the sample prepared with 42.9 vol.% water–ethanol mixed solution consisted of mixture of anhydrous tungsten oxide and hydrous one. It may also play an important role in improving the photocatalytic activity, since the heterogeneous electron transfer to retard quick recombination of photo-induced electron and hole can be expected.

4. Conclusion

Tungsten oxides with different morphologies and crystal phases were successfully synthesized by solvothermal reaction. The morphology and crystal phase of tungsten oxides could be effectively controlled by the adjustment of the solvents in reaction. Micro-sized spherical particles and bundles consisting of nanowires of tungsten oxides were obtained when using ethanol and 1-propanol as solvents, respectively. When water–ethanol mixed solution was used, tungsten oxides with higher crystallinity and lower band gap energy could be obtained. The sample prepared with 42.9 vol.% water–ethanol mixed solution was a mixture of anhydrous tungsten oxide and hydrous one, which showed preferential orientation of (0 0 2) plane and higher photocatalytic activity despite of their relatively small specific surface area. As a result, it can be reasonably deduced that compared with specific surface area, the crystallinity had more important effects on the photocatalytic activity of tungsten oxides in the test of nitrogen monoxide destruction.

Acknowledgment

This work was supported by the Ministry of Education, Culture, Sports, Science and Technology, Japan, Special Education and

Research Expenses on "Post-Silicon Materials and Devices Research Alliance".

References

[1] S.J. Yoo, Y.H. Jung, J.W. Lim, H.G. Choi, D.K. Kim, Y.E. Sung, Sol. Energy Mater. 92 (2008) 179.
[2] D.M. Satoca, L. Borja, A. Rodes, R. Gomez, P. Salvador, Chem. Phys. Chem. 7 (2006) 2540.
[3] A.A. Ashikarran, A. Iraji zad, M.M. Ahadian, S.A. Mahdavi Ardakani, Nanotechnology 19 (2008) 195709.
[4] Y.S. Kim, Sens. Actuators B 137 (2009) 297.
[5] H. Takeda, K. Adachi, J. Am. Ceram. Soc. 90 (2007) 4059.
[6] J. Polleus, A.A. Gurlo, N. Barsan, U. Weimar, M. Antonietti, M. Niederberger, Angew. Chem. 118 (2006) 267.
[7] J.Ch. Yang, P.K. Dutta, Sens. Actuators B 136 (2009) 523.
[8] I.M. Szilagyi, L. Wang, P.I. Gouma, C. Balazsi, J. Madarasz, G. Pokol, Mater. Res. Bull. 44 (2009) 505.
[9] C. Balazsi, L. Wang, E.O. Zayim, I.M. Szilagyi, K. Sedlackova, J. Pfeifer, A.L. Toth, P.I. Gouma, J. Eur. Ceram. Soc. 28 (2008) 913.
[10] C.S. Rout, M. Hegde, C.N.R. Rao, Sens. Actuators B 128 (2008) 488.
[11] On. Nimittrakoolchai, S. Supothina, Mater. Chem. Phys. 112 (2008) 270.
[12] S. Luo, G. Fu, H. Chen, Zh. Liu, Q. Hong, Solid State Electron. 51 (2007) 913.
[13] Zh.G. Zhao, M. Miyauchi, Angew. Chem. 120 (2008) 7159.
[14] R. Abe, H. Takami, N. Murakami, B. Ohtani, J. Am. Chem. Soc. 130 (2008) 7780.
[15] T. Arai, M. Horiguchi, M. Yanagida, T. Gunji, H. Sugihara, K. Sayama, Chem. Comm. (2008) 5565.
[16] Z.G. Zhao, M. Miyauchi, Angew. Chem. Int. Ed. 47 (2008) 7051.
[17] D.N. Ke, H.J. Liu, T.Y. Peng, X. Liu, K. Dai, Mater. Lett. 62 (2008) 447.
[18] A. Watcharenwong, W. Chanmanee, N.R. de Tacconi, C.R. Chenthamarakshan, P. Kajitvichyanukul, K. Rajeshwar, J. Electroanal. Chem. 612 (2008) 112.
[19] Y. Guo, X. Quan, N. Lu, H. Zhao, Sh. Chen, Environ. Sci. Technol. 41 (2007) 4422.
[20] H. Kominami, J. Kato, Sh. Murakami, Y. Ishiii, M. Kohno, K. Yabutani, T. Yamamoto, Y. Kera, M. Inoue, T. Inui, B. Ohtani, Catal. Today 84 (2003) 181.
[21] R. Hu, H. Wu, K. Hong, J. Cryst. Growth 306 (2007) 395.
[22] S. Supothina, P. Seeharaj, S. Yoriya, M. Sriyudthsak, Ceram. Int. 33 (2007) 931.
[23] S.B. Sun, Y.M. Zhao, Y.D. Xia, Z.D. Zou, G.H. Min, Y.Q. Zhu, Nanotechnology 19 (2008) 305709.
[24] G. Wang, Y. Ji, X. Huang, X.Q. Yang, P.I. Gouma, M. Dudley, J. Phys. Chem. B 110 (2006) 23777.
[25] Z. Gu, T. Zhai, B. Gao, X. Sheng, Y. Wang, H. Fu, Y. Ma, J. Yao, J. Phys. Chem. B 110 (2006) 23829.
[26] Y. Baek, K. Yong, J. Phys. Chem. C 111 (2007) 1213.
[27] H.G. Choi, Y.H. Jung, D.K. Kim, J. Am. Ceram. Soc. 88 (2005) 1684.
[28] J.H. Ha, P. Muralidharan, D.K. Kim, J. Alloys Compd. 475 (2008) 446.
[29] X.C. Song, Y.F. Zheng, E. Yang, Y. Wang, Mater. Lett. 61 (2007) 3904.
[30] D. Chen, J.H. Ye, Adv. Funct. Mater. 18 (2008) 1922.
[31] S. Yin, K. Ihara, R. Li, T. Sato, Res. Chem. Intermed. 34 (2008) 393.
[32] S. Yin, M. Komatsu, B. Liu, R. Li, Y. Wang, T. Sato, J. Mater. Sci. 43 (2008) 2240.
[33] Z.G. Zhao, M. Miyauchi, J. Phys. Chem. C 113 (2009) 6539.
[34] H. Kominami, J. Kato, S. Murakami, Y. Ishii, M. Kohno, K. Yabutani, T. Yamamoto, Y. Kera, M. Inoue, T. Inui, B. Ohtani, Catal. Today 84 (2003) 181.
[35] S. Yin, T. Sato, Ind. Eng. Chem. Res. 39 (2000) 4526.